Novel Synthesis and Characterization of Doxycycline-Loaded Gold Nanoparticles: The Golden Doxycycline for Antibacterial Applications

Maroua Ben Haddada, Katy Jeannot, Jolanda Spadavecchia

DOI: 10.1002/((please add manuscript number))
Article type: (Full Paper)

Novel synthesis and characterization of doxycycline-loaded gold nanoparticles. The golden doxycycline for antibacterial applications.

Maroua Ben Haddada[1], Katy Jeannot[2], Jolanda Spadavecchia[1]*

[1] *CNRS, UMR 7244, CSPBAT, Laboratoire de Chimie, Structures et Propriétés de Biomateriaux et d'Agents Therapeutiques Université Paris 13, Sorbonne Paris Cité,* Bobigny, *France*

[2] *Laboratoire de Bactériologie, Centre National de Référence (CNR) de la Résistance aux Antibiotiques, Centre Hospitalier Régional Universitaire (CHRU) de Besançon, UMR4269 "Chrono-Environnement", Boulevard Fleming, 25030 Besançon, France.*

ABSTRACT

Doxycycline (DOXY) is a tetracycline antibiotic with a potent antibacterial activity against a wide variety of bacteria. One potential strategy to enhance the penetration and the antibacterial activity of antibiotics is the use of nanotechnology. In this work, we report an innovative synthesis of a stable PEG-AuNPs loaded with DOXY. To the best of our knowledge, this is the first report on the combination of DOXY with gold nanoparticles as polymeric complex. The obtained nanoparticles were fully characterized by transmission electron microscopy (TEM), dynamic light scattering (DLS), zeta-potential, UV-Vis and Raman spectroscopy. The stability and sustained activity of the drug in nanoparticles was determined on a panel of Gram positive and Gram negative bacteria in comparison with the native form of the drug. This combined therapeutic agent restored the susceptibility of DOXY and showed an antibacterial activity against major human pathogens (*Staphylococcus aureus*, *Escherichia coli*, *Klebsiella pneumoniae*, *Pseudomonas aeruginosa*, and *Acinetobacter baumannii*). Synergy of antibiotic with nanoparticles is quite promising, notably for antibiotic resistant strains. The antibacterial effect of combination of DOXY with gold nanoparticles was conserved despite the production of antibiotic resistance mechanisms in all the strains tested. Doxycycline-loaded nanoparticles could be used efficiently for antibacterial therapy, possibly against a large number of bacterial species.

KEYWORDS: AuNPs, doxycycline, antibiotic conjugation, antibacterial effect.

1. INTRODUCTION

Antibiotic resistance has been compared to as *"the silent tsunami facing modern medicine"*[1]. The broad use and the improper administration of antibiotics had make bacteria able to develop resistance against them. Many conventional antimicrobials became obsolete due to the emergence of multidrug-resistant pathogens [1]. The chemical modification of antibiotic scaffolds to evade overcome bacterial resistance and to synthesize new antibiotics of high efficiency is time consuming and is often not economically feasible. Moreover, the antibiotic dosage often prescribed in some therapy is much higher leading to harmful side effects. For a successful antibiotic therapy, the antibiotic dose should be reduced and the stability should be increased to make the usage economical. One potential strategy to overcome this problem is the use of nanotechnology [2]. Several studies have reported the antimicrobial activity of antibiotics conjugated with different nanoparticles [3] [4] [5] [6] [7].The combination of antibiotics to inorganic nanoparticles might enhance their antimicrobial effectiveness against multidrug resistant bacteria[8]. Moreover, nanoparticles were shown to take up by phagocytic cells that improves the delivery of antibiotics for the treatment of intracellular infections[9].

Gold and silver nanoparticles, as drug carriers, possess the potential to increase drug concentration at infected sites, combat its side effects and target the drug to the appropriate site of action[10]. As examples, Gu et *al.* have reported the enhanced antimicrobial activity of vancomycin coated gold nanoparticles on vancomycin resistant enterococci [11]. Saha et *al.* demonstrated that the *in vitro* bactericidal activity of gold nanoparticles conjugated ampicillin, streptomycin and kanamycin were more efficient compared to their respective free forms[12].

Deng et *al* have shown the synergic effect of amoxicillin with silver nanoparticles against *Escherichia coli*[13]. Rai et al. used cefaclor as both reducing and capping agent to produce spherical gold nanoparticles and showed a potent activity against both Gram-positive and Gram-negative bacteria[3]. Doxycycline (DOXY) (**Scheme S1 Supporting Informations**) has

been recognized as a family of tetracycline antibiotics of very efficient antimicrobial activity[14] [15]. The chemical structure of DOXY is very similar to doxorubicin (DOX)[16]. Both molecules contains a tetracyclic molecule, including planar and aromatic hydroxyl anthraquinone rings, which function as chromophore, responsible for therapeutic activity[17] [14]. However, the formulation in use has shown dramatic side effects as their low bioavailability[15], is responsible for delivery problems and consequently of systemic toxicity that limited their medical application[18]. Recently, J. Spadavecchia et al. have synthetized an original nanovector based on doxorubicin-gold-complex, by a chelation reaction in which, the drug was complex with tetrachloauric acid ($HAuCl_4$) and polymer molecules before reduction to final nanovector (DOX IN AuNPs) [16] . The same authors have also studied the mechanism of hybrid nanoparticles using doxorubicin capped onto gold nanoparticles with biocompatible polymers as capping agent (DOX-ON AuNPs) in order to compare the different activity of both nanovectors [19] [20], and their remarkable interest in therapeutic activity to *in vitro* model of Pancreatic Ductal Adeno Carcinoma (PDAC)[19] [16].

In this paper, we combined gold nanoparticles (AuNPs) with DOXY by three chemical different methodologies (DOXY-AuNPs, DOXY ON-AuNPs, DOXY IN-AuNPs) and, evaluated the antimicrobial effect of these hybrids on several bacterial species in the presence of gold nanoparticles (AuNPs) synthetized. Therefore, the development of a simple and fast method to improve the activity of DOXY and oxytetracycline has become increasingly attractive [13].

The combination DOXY ON AuNPs exhibited the lower MICs (≤ 2 mg/L) in comparison with native DOXY in all species tested. Interestingly, the DOXY ON AuNPs was stable against the major resistance mechanisms to antibiotics acquired by human pathogen bacteria.

2. RESULTS AND DISCUSSION

Formation mechanism and physico-chemical characterization of Doxycycline Nanoparticles (DOXY-Au NPs, DOXY IN-Au NPs, DOXY ON-Au NPs,)

In the last years many authors have produced antibiotic mediated synthesis of gold and silver nanoparticles with potent antimicrobial activity and their application in antimicrobial coatings [3].

Other authors have designed a nanocomposite based on DOXY -loaded polymeric nanoparticles in order to improve drug delivery and efficacy with considerable antimicrobial activity[6] [21] . In our case, the synthesis of DOXY-AuNPs (**Scheme 1 A**) was carried out at room temperature by reduction of gold ions ($AuCl_4^-$) using DOXY as reducing and capping agent on the growth process. A fast reduction in the time of gold ion, was observed when the reaction was performed at room temperature under basic conditions (NaOH). It is well established that amine and carbonyl groups can easily chelate and transfer electrons to gold ions (Au^{3+}), leading to the formation of Au^0 (nuclei)/ Au–amine complexes via simple amine-carbonyl chemistry[16] [22] [23]. Pending the reduction of gold ions ($AuCl_4^-$) exploiting DOXY drives to a rise in the rate of reduction of the gold ions, which favors an enhanced nucleation rate with the formation of a gold grains[24] [25]. Gold ions are consequently reduced on the surface of gold nuclei, therefore involving the achievement of spherical gold nanoparticles of smaller sizes, which are embedded and stabilized by DOXY (**Scheme 1 A and scheme 2**). In order to improve the stability and biological activity of the gold nanoparticles in object, we decided to apply some modification to original synthesis, through the methodology ON and IN extensively described by J.Spadavecchia *et al.*[19] [16] [26] [27]

Scheme 1 B showed a chemical procedure, named methodology IN, in which DOXY and PEG both participate actively to the stabilization of AuNPs via chelation between their chetone and amino groups with chloride auric ions. Chelation sites include the β-diketone

system (positions 11 and 12) , the enol (positions 1 and 3) and carboxamide (position 2) groups of the A ring (**see figure S1)**[28].

The stacking process by electrostatic interaction between polymer (PEG) and DOXY-Au complex and final reduction in the presence of $NaBH_4$ are responsible of final growth process and colloidal stabilization as previously described[16] [26] (**scheme 1B**). The third synthetic protocol, named methodology ON was depict in **scheme 1C** and performed in two main steps**:** 1) firstly, PEG-capped AuNPs were synthetized (**PEG-AuNPs**) and 2) further conjugated to DOXYL by carbodiimide chemistry between carboxylic group of PEG diacide onto AuNPs and amino group of DOXY as schematically showed. Based on our chemical design, the PEG-AuNPs appertain to the category of nanomedicines in which the drug payload is promptly conjugated to the nanoparticle surface *via* degradable covalent bond [19]. The amide group binding the PEG chains to the DOXY molecules was designed so that it could be cleaved under the specific conditions in the cytoplasm releasing the drug in protonate form [5, 29]. At present it is recognized that the efficacy of antibacterial drugs is in many cases hampered by low antimicrobial concentration due to their poor bioavailability at the disease site.

All nanoparticles of our chemical procedure were extensively characterized by UV-Vis absorption spectroscopy, TEM and Raman spectroscopy. When DOXY was mixed to the $AuCl_4^-$ solution, in the presence of NaOH, the formation of spherical gold nanoparticles (**DOXY-AuNPs**) of about 6.5 ± 0.7 nm was observed by TEM **(Figure 1B-a)**.

UV-Vis absorption spectroscopy analysis of **DOXY-AuNPs** products (**Figure 1A; dark cyan**) showed a clear band at 530 nm. The band positions are compared with spectroscopic band observed with individual DOXY molecules. This means that the DOXY could be present inside the solution as well as another compound. Moreover, the individual DOXY exhibits two pronounced UV-Vis absorption peaks at 346 nm and 274 nm. This

spectroscopical finger print was associated to π-π* electronic transitions due to interactions between the DOXY ring and $AuCl_4^-$ ions[30] making a clear demonstration of the complex formation. In agreement with previously studies[16] [26] [27], we arrogate that this band is due to electronic delocalization of aromatic ring and HOMO-LUMO transition and clear up that DOXY was really involved into the nucleation process and builds a complex with Au.

In the case of **DOXY IN-AuNPs** synthesis, PEG molecules improved the reduction process by interacting with the DOXY-$AuCl_4^-$ complex, stabilizing such complex and subsequently acting as surfactant in the nucleation and growth of the nanostructures. In particular, the formation of gold nanoparticles from $AuCl_4^-$ can be recapitulated in three steps (**see scheme 3**):

(1) Formation of DOXY-PEG diacid complex; (2) initial reduction of metal ions improved by DOXY and dicarboxylic acid-terminated PEG in aqueous solutions to form gold clusters; (3) adsorption of DOXY-PEG diacid complex on the surface of gold clusters and reduction of metal ions in that vicinity with consequently growth of gold particles and colloidal stabilization by molecules of PEG polymers.

Interactions between $AuCl_4^-$ ions and mixture of DOXY-PEG diacid molecules (attractive ion-dipole interactions *vs* repulsive interactions due to hydrophobicity) are decisive in order to check the competition between $AuCl_4^-$ reduction, and the final particle size [31].

DOXY IN-AuNPs absorption spectrum exhibits a small peak at 310 nm and a second one centered at 540 nm (**Figure 1A red line**). This latter peak is assigned to the localized surface plasmon of the nanoparticle with diameter of 23 nm embedded in PEG environment as expected [32]. The AuNPs thus formed were characterized by TEM and have spherical shape (**Figure 1B-b)** with a diameter close to 23 ± 4.2 nm, confirmed by the hydrodynamic

diameter measured by zetasizer (**Table 1 in Supporting Information**). Previously J.Spadavecchia *et al.* have reported the synthesis of similar nanostructures using dicarboxylic PEG [31, 33] [34] obtaining PEG AuNPs as building block of nanovectors [19] [16] [26] [27] .

On the basis of previous studies, when DOXY was conjugate to PEG AuNPs by carbodiimide chemistry to form **DOXY ON-AuNPs**, we obtain a nanoconjugate in which DOXY was grafted on the surface of polymer-nanoparticle, taking on a different chemical and conformation (**see scheme 4**) . We observe a red shift plasmon peak from 515 nm relative at PEG AuNPs (**Figure 1 A –black line**) to 525 nm (**Figure 1 A –green line**) with a different chemical and steric arrangement between PEG and DOXY onto the surface of AuNPs that influences the final size of the nanoparticles.

TEM images show spherical gold nanoparticles with a mean diameter of about 13 nm ±1.2 nm (**Figure 1B-c).** In addition, the bright red color of the obtained nanoparticles and the UV-Vis spectra remain unaltered after storage for more than three months at room temperature validating the formation of stable particle suspension.

The Raman spectra of free DOXY (control) , DOXY-AuNPs, DOXY IN-AuNPs and DOXY ON-AuNPs in water exhibit many bands in the region 400-2000 cm^{-1} **(Figure 2)**. The wide band observed around 1600 cm^{-1} on the raman spectra is assigned to the water. The bands for DOXY (**Figure 2 blue line**) were assigned in the following manner: frequencies at 1677 cm^{-1} and 1537 cm^{-1} are related to the carbonyl and amino groups of the amide, respectively, in ring A; bands at 1613 cm^{-1} and 1581 cm^{-1} correspond to the carbonyl groups in rings A and C, respectively; the band at 1458 cm^{-1} is related to the C=C skeleton vibration. The oxygen atoms on C1 and C3 may be equivalent because there was only one frequency at 1615 cm^{-1}. The triplet peak at 430-459-493 cm^{-1} is due to the vibrations δ (OH…O), ν (OH…O) of the DOXY molecule. For instance, a double peaks at 1312 - 1270 cm^{-1} and 1175 cm^{-1} was assigned to C=O carbonyl stretching and C-O-C stretching in backbone of DOXY. When

DOXY chelate to Au^{3+} to form **DOXY-AuNPs** (**Figure 2 - dark cyan**) in alkaline medium, we observed an apparition of the peaks at 1386 cm^{-1} due to C-O plane deformation of amide group, 1542 cm^{-1} assigned to ν C-C stretching and a strong peak at 882 cm^{-1}, due to C=O group of quinolone. For instance, a double peak at 1312-1270 cm^{-1} is lowered. A triplet peak in the spectral region 430-493 cm^{-1} disappeared. These bands are due to variation of the steric conformation of the DOXY and become more prominent upon complexation, as described previously[33a] [34]. These results were in part confirmed in **DOXY IN-AuNPs**, in which DOXY chelate to Au^{3+} in the presence of PEG diacid to form hybrid nanoparticles. The raman spectra clearly shows band changes of amide carbonyl and amino groups in ring A. **Figure 2 red line** showed an apparition of the peaks at 1423 cm^{-1},1370cm^{-1}, 1284 cm^{-1}, due to C-O plane deformation of carboxylic acid, and C=O carbonyl stretching of the PEG . However, the peaks for amide C=O of DOXY shifted from 1625-1657 cm^{-1} to 1633 cm^{-1} and those of $–NH_2$ shifted from 1579 cm^{-1} to 1536 cm^{-1}. These results suggest that the interaction of DOXY with PEG could take place through the amide C=O in ring A. A similar steric conformation of DOXY in hybrid nanoparticles (**DOXY IN-AuNPs**) compared to DOXY AuNPs was confirmed by a disappearance of triplet peak in the region 400-430 cm^{-1}. These bands were assigned to DOXY aromatic rings vibrations and to those of C=O and hydroxyl groups in the DOXY molecule. It is already previously described that most of the Raman bands of molecules can be significantly increased by their proximity to the surface AuNPs[16]. Thus, the enhancement of such bands is herein demontrated as a trial of the drug loading into AuNPs, as well as to their arrangement within the particles. When DOXY was grafted onto PEG-AuNPs, by carbodiimide chemistry to form DOXY ON AuNPs (Figure 2 green line), a strong spectroscopic variation was occurs. In particular we observed a SERS effect in the region 400-2000 cm^{-1}. A double peak at 1462-1438 cm^{-1} is due to vibration N-H ; the increase of the peaks at 1364-1318-1275 cm^{-1} is due to a different C-O plane deformation of

carboxylic acid, and C=O carbonyl stretching of the PEG backbone. This result was confirmed by the shift of the peak from 1175 cm^{-1} to 1182 cm^{-1}, due to C-O-C vibration. The steric and chemical conformation of DOXY onto the surface of PEG AuNPs was demonstrated by a strong SERS effect in the peak at 982 cm^{-1} due to C-O plane deformation in the ring of DOXY and the apparition of triplet peaks in the region 430-500 nm due to the vibrations δ(OH…O), ν(OH…O) of the DOXY molecule. Based on these findings, we conclude that DOXY assumes three different chemical conformations on the basis of chemical protocol to form hybrid nanoparticles.

Stability of DOXY gold nanoparticles (DOXY-AuNPs, DOXY IN-AuNPs, DOXY ON-AuNPs):

The stability of **DOXY gold nanoparticles** in solution, pivotal a significant role in the clinical purposes[35] and was monitored by the Localized Surface Plasmon (LSP) band of the synthetized AuNPs (**scheme 1; Figure 1**). Analysis was performed at pH 8 and electrolytic conditions over a reasonable period of time (3 months). The synthesized AuNPs did show an almost negligible change in the LSP band position over a period of three- months at the pH 8 (**Figure S1** in the Supporting Information). The decrease in intensity of plasmon peak, is due to agglomeration phenomena owing the oxidation process. **Zeta potential measurements confirmed the spectroscopic results, showing that DOXY ON-AuNPs and DOXY-AuNPs were colloidally stable at physiological pH (z-potential = -25 ± 0.5 mV and z-potential = -34 ± 0.8 mV with a PdI equal to 0.3) (Table 1). We suggest that DOXY ON-AuNPs enhanced stability was associated with the presence of the PEG coating. The zeta potential of DOXY IN -AuNPs products in fact was found equal to -17.93 ± 0.7 mV, indicating a mild dispersion. The negative zeta potential suggested the presence of free negative charges in the sample, probably associated to free chloride ions (Cl^-) and/or**

ionisable functions, such as the phenolic groups on the DOXY molecules present in the Au (III)-DOXY complexes.

Drug loading and release of DOXY Nanoparticles (DOXY-Au NPs, DOXY IN-Au NPs, DOXY ON-Au NPs):

Previously, A. Kumar et al. have studied the process of loading of DOXY onto chitosan nanoparticles to improve drug delivery and treatment efficacy[6] .The effectiveness of a gradient loading system is highly dependent on the chemistry of the drug being loaded[36]. Gradient-loading systems in response to a pH gradient, have been developed for other antibacterial drugs, **but differ from the method described** in the current manuscript. We developed a novel loading methodology, resulting in pegylated nanoparticles with higher drug loading and longer retention times than passive aqueous capture[37]. Our loading efficiency is 10–40 times more efficient than the previously published methods [36] [6] .

Previous formulations of DOXY in DPPC/cholesterol liposomes used mannose or glucose solutions at a pH of 6.0 as non ionic hydrating solutions, and these formulations have encapsulation efficiencies of nearly 10-fold less than the sulfuric acid–loading technique[38]. The percentage of released drug is dependent on the initial drug concentration, and equilibrium between the soluble drug and precipitate follows a zero-order process if the drug precipitates in the liposome[39]. Tu et al. used an ammonium sulfate gradient–loading system to describe the liposomal loading of the drug based on the amount of ammonium ion in the liposomes and the initial amount of drug added[40].

The successful loading ratio of DOXY onto PEG-AuNPs (**DOXY ON-AuNPs**) and complexed with $AuCl_4^-$ and PEG diacid (DOXY-AuNPs, DOXY IN-AuNPs) were evidenced by the characteristic absorption peaks at 273 nm and 345 nm from DOXY **(Figure S2-A Supporting information)**. The standard absorption of DOXY was plotted in the inset of

figure **(Figure S2-B Supporting information)** according to UV-Vis absorbance spectra of DOXY at various concentrations. The loading efficiencies were estimated to be 86% with 8.7 µg present in 2.7×10^{-8} mol of NPs (data not shown) for DOXY ON-AuNPs, 65% for DOXY IN-AuNPs, and 54% for DOXY-AuNPs. DOXY releases were pH- and time-dependent (**Figure 3 A-B**). A sustained drug release was observed in the first 5 h for both drugs at pH 5 and 8, which is highly favorable for drug delivery as the bacterial thrive in basic conditions. We presumed that the release of DOXY was checked by a ionic equilibrium between Au (III)-PEG complexes trapped into AuNPs by the hydrophobic interactions between PEG chains and ionic drug. As previously described, the mechanism by which basic pH triggers drug release is probably associated to the presence of carboxylate groups in the chemical structure of PEG molecules. Such groups become dissociated in anionic form at basic pH. This improve the electrostatic interactions occurring between PEG and drugs that stabilize the DOXY ON AuNPs structure.

We suppose that, the ionic strength and anionic form of DOXY onto PEG chains improve the water solubility of the drug molecules, taking advantage of the drug release from AuNPs. Indeed, a remarkable moiety of DOXY electrostatically binding onto dissociated complex is released, through PEG chain and diffusion phenomena [33a, 41].

Extended spectrum of DOXY ON-AuNPs activity in bacteria

It is well established that tetracyclines inhibit bacterial protein synthesis by preventing the association of aminoacyl tRNA with the bacterial ribosome[42] [43]. Therefore, to interact with their targets these molecules need to traverse one or more membrane systems depending on whether the susceptible organism is gram positive or gram negative. The extensive structure-activity studies have demonstrated that, the membrane-disrupting properties of the atypical tetracyclines are probably related to the relative planarity of the B, C, and D rings so that a

lipophilic, non ionized molecule predominates. On interaction with the cell, the atypical tetracyclines are likely to be preferentially trapped in the hydrophobic environment of the cytoplasmic membrane, disrupting its function [43] .

The presence of surfactant molecules onto the surface of nanoparticles, are usually undesirable , due to their capacity to block adsorption sites[5]. Heloiza F. O. Silva et al. have showed, that polyvinyl alchol (PVP), play a key role in linking with DOXY onto silver nanoparticles (AgNPs)[5]. They demonstrated, that less silver to be released, due to the layer size of the AgNPs and consequently, DOXY can release more easily followed the disruption of ATP production and an increase in DNA mutation[44].

However, we have shown that PEG diacid played a paramount role in concentrating DOXY around the particle, which culminated in an increased bacteriostatic activity. To evaluate the antibacterial activity of the synthetized nanoparticles, we selected a panel of bacteria frequently involved in clinical infections, including Gram positive and Gram negative bacteria (**Tables 1, and 2**). The MICs of compounds were compared with reference antibiotics (amoxicillin, ceftazidime, and imipenem). Whichever the bacteria tested the lowest MICs was measured in presence of DOXY ON-AuNPs (**Tables 1, and 2**). The MICs of DOXY ON-AuNPs were 8 to 16 fold lower than that unmodified DOXY in Gram positive and negative, even in **DOXY** intrinsically resistant bacteria like *P. aeruginosa*. It is worth noting that the MIC values of DOXY ON-AuNPs were similar to that of reference antibiotics such as amoxicillin in *S. aureus* (ATCC®25923™), and *E. faecalis* (JH2-2), and ceftazidime in *P. aeruginosa* (PAO1) and *A. baumannii* (CIP7010). Whereas the DOXY-AuNPs did not display antibacterial activity, the DOXY IN-AuNPs possessed a poor activity against Gram positive and negative bacteria. According to these results, we focused the susceptibility tests with DOXY ON-AuNPs, and DOXY IN-AuNPs. As antibiotic resistance is becoming a global critical issue particularly in ESKAPE pathogens including the species *E. coli*, *S. aureus*,

K. pneumoniae, *A. baumannii*, *P. aeruginosa*, and *E. aerogenes* [45], we determined the MICs of DOXY ON-AuNPs, and DOXY IN-AuNPs in several ESKAPE pathogens, which were resistant to antibiotics by producing the most prevalent antibiotic resistance mechanisms in clinical isolates. While the *S. aureus* ATCC®700699™ strain produces a PLP-2a responsible for resistance to methicillin (MRSA), the addition of ON-AuN, restored the susceptibility to DOXY (from >32 mg/L to 2 mg/L) as in susceptible strain ATCC®25923™ (**Table 1**). Similarly, resistance to amoxicillin and vancomycin due to a modification of the PBP-5 and the acquisition of the transposon Tn*1546* respectively, did not modify the susceptibility to DOXY ON-AuNPs (MIC = 2 mg/L) in strain BM4147[46]. All these data suggest that the MIC of DOXY ON-AuNPs is not affected by the most prevalent resistance mechanisms in Gram positive bacteria.

Activity of *DOXY IN-AuNPs and DOXY ON-AuNPs* on *P. aeruginosa*

P. aeruginosa is the most frequently pathogen in health care associated pneumonia infections in Europe [47]. As few molecules are active on *P. aeruginosa* strains due to the production of several intrinsic resistance mechanisms, and its capacity to easily acquired mutations and foreign DNA, we assessed the impact of several resistance mechanisms to antibiotics on the activity of DOXY IN-AuNPs and DOXY ON-AuNPs [48].

P. aeruginosa naturally produces an inducible cephalosporinase, AmpC, that may be overexpressed due to mutations in regulatory pathways genes (*dacB*, *ampG*)[49]. Overproduction of AmpC contributes to ceftazidime resistance, an antibiotic belonging to β-lactams family and usually used in first line of treatment of *P. aeruginosa* infections. As, the prevalence of AmpC mutants is high in clinical stains, we determined the MIC of DOXY IN-AuN and DOXY ON-AuNPs in previously AmpC overproduction well-characterized clinical strains (**Table 3**) in comparison with that of ceftazidime. While the DOXY IN-AuNPs was more active (MIC from 4 to 8 mg/L) than DOXY (32 mg/L) like in susceptible strain PAO1,

it remained less active than DOXY ON-AuNPs. In the five clinical strains (5134, 5168, 5250, 5257, and 5268), the MICs of DOXY ON-AuNPs were identical (2 mg/L) and similar to the MIC of the susceptible strain PAO1 (2 mg/L) (**Table 2, and 3**) indicating that the activity of DOXY ON-AuNPs is not compromised in strains overproducing AmpC. However, *P. aeruginosa* may acquire additional β-lactam resistance mechanisms, notably by the production of enzymes hydrolyzing these molecules (β-lactamases) including Extended Spectrum β-lactamases (ESBL), and carbapenemases. ESBL (Ambler class A β-lactamases) and carbapenemases (Ambler class B, metallo-β-lactamases) have been largely reported in *P. aeruginosa* and have worldwide diffused [50].These enzymes contribute to the emergence of Multi-Drug Resistance strains (MDR), and eXtensively Drug Resistant strains (XDR)[51]. Whereas the strains were highly resistant to ceftazidime (MIC from 16 to>64 mg/L) and/or imipenem (MIC from 2 to >64 mg/L), the last therapeutic option in β-lactams, the MICs of DOXY ON-AuNPs were not modified in strains producing ESBL (VEB-1a, SHV-2a, GES-1, and PER-1) or carbapenemases (VIM-2, IMP-13, IMP-15, and NDM-1). All these data show that DOXY ON-AuNPs is stable and is not affected (from 0.5 to 2 mg/L) by the major antibiotic resistance mechanisms identified in *P. aeruginosa* clinical strains. These promising results suggest that further studies with AuNPs combined with antibiotics are an interesting approach to challenge antibiotic resistance.

Hypothetical mechanisms for antimicrobial activity of DOXY gold nanoparticles :

There are many reports on the mechanism of antimicrobial activity of metallic nanoparticles. Unfortunately, the exact mechanism by which nanoparticle inhibits the growth of organism has not been well expounded. It was described by literature[3] , that gold nanoparticles interact with the outer membrane of the bacteria through porin channels, and then accumulate on the membrane bilayer matrix, thanks their interaction with lipopolysaccharide and protein [52] damaging the membrane integrity. This behavior could explain the low antibacterial activity

of gold nanoparticles. Although the mechanism behind the activity of DOXY hybrid nanoconjugate are not yet fully clarified, we suggest that the antibacterial activity of DOXY ON-AuNPs is more better than , DOXY IN- AuNPs and DOXY-AuNPs, compared to DOXY *free* as control. We believe that after conjugation of DOXY onto AuNPs, by EDC/NHS through PEG-COOH chains, DOXY was protonated and migrate through the PEG chains, assuming a favorite steric conformation to diffuse more freely in the cytoplasm as DOXY molecule charged positively, blocking the binding of aminoacyl-tRNA to the mRNA-ribosome complex (**scheme 4**).

The mechanism of enhanced antibacterial activity and advantages of DOXY reduced gold nanoparticles (DOXY-AuNPs) (scheme 5 A) can be explained as follows: DOXY reacts with the outer peptidogylcan layer of Gram-positive bacteria thereby increasing the membrane's permeability, generation of reactive oxygen species (ROS) with oxidative deterioration to cell content. Subsequently, uptake of ions derived from nanoparticles, ATP production, and inhibition of DNA replication [52]. Therefore, the combined action of DOXY and Au nanoparticles leads to enhanced antibacterial activity due to relase as DOXY-Au complex negatively charged.

Contrarily, in the formulation DOXY IN-AuNPs, DOXY chelate Au(III) to form a complex before the staking process of PEG diacid chains; in this configuration, DOXY assume a different steric arrangement, in which hydriquinone and chetone groups in the ring B-C chelate Au ions before reduction with $NaBH_4$ to form AuNPs. In this formulation, DOXY was released in the cytoplasm as DOXY-Au complex through migration in the PEG chains with evident variation in driven force and electrolytic condition **(scheme 5B**).

Table 1. Susceptibilities of Gram positive bacteria.

	MIC (mg/L)				
Species	*Staphylococcus aureus*		*Enterococcus faecalis*	*Enterococcus faecium*	
Name of reference strains	ATCC® 25923™	ATCC® 700699™	UCN41	BM4147	ATCC® 19434T™
DOXY	32	>32	>32	32	32
DOXY NP-AuNPs	32	32	32	32	32
DOXY IN-AuNPs	8	4	4	4	4
DOXY ON-AuNPs	1	2	2	2	2
Amoxicillin	1	8	1	8	1

Table 2. Susceptibilities of Gram negative bacteria.

	MIC (mg/L)			
Species	*E. coli*	*Klebsiella pneumoniae*	*Pseudomonas aeruginosa*	*Acinetobacter baumannii*
Name of reference strains	ATCC® 25922™	ATCC® 700603™	PAO1	CIP7010
DOXY	2	32	32	16
DOXY NP-AuNPs	>32	>32	>32	32
DOXY IN-AuNPs	8	4	8	4
DOXY ON-AuNPs	2	2	2	2
Amoxicillin	0.12	>8	>256[a]	>256[a]
Ceftazidime	<0.12	0.12	2	2

[a] Bacteria intrinsically resistant to amoxicillin.

Table 3. Susceptibilities of *P. aeruginosa* clinical strains producing various β-lactamases.

	MIC (mg/L)														
Name of clinical strain	5134	5168	5250	5257	5268	5213	5231	5242	5176	5099	4925	5190	5225	5264	5269
Resistance mechanism	Strains overproducing the chromosomal cephalosporinase AmpC					Strains producing a metallo-β-lactamase, carbapenemases						Strains producing an ESBL[a]			
						VIM-2			IMP-13	IMP-15	NDM-1	VEB-1a	SHV-2a	GES-1	PER-1
DOXY	32	32	32	32	32	>32	32	32	32	32	32	32	32	>32	32
DOXY IN-AuNPs	8	8	8	8	4	8	8	8	4	32	8	32	8	8	8
DOXY ON-AuNPs	2	2	2	2	2	2	2	2	2	0.5	2	0.5	2	2	2
Ceftazidime	32	4	64	4	>64	>64	>64	16	>64	64	>64	>64	16	>64	>64
Imipenem	2	2	2	2	2	>64	>64	32	>64	16	>64	4	>32	2	>64

[a] ESBL, Extended Spectrum-β-lactamase.

3. EXPERIMENTAL SECTION

Materials

Tetrachloroauric acid ($HAuCl_4$), sodium borohydride ($NaBH_4$), N-hydroxysuccinimide (NHS), 1-(3-dimethylaminopropyl)-N′-ethylcarbodiimidehydrochloride (EDC), PEG-600 diacid, doxycycline hydrochloride (DOXY), bacterial culture media, was purchased from Sigma-Aldrich (St Louis, MO, USA). All solvents were reagent-grade and used without any further purification. All bacteria were provided by Laboratoire de Bactériologie, Centre National de Référence (CNR) (France). Experiments were carried out at room temperature if not specified otherwise.

Preparation of Nanoparticles

Three strategies of synthesis were tested to conjugate DOXY to AuNPs:

Doxycycline reducing and formation of DOXY-AuNPs

DOXY-AuNPs were synthesized by mixing 20 mL of $HAuCl_4$ solution (8.63×10^{-4} M) with 4 mL of DOXY (1mg/mL) followed by the addition of 3 mL NaOH (1mM). After 15min of reaction, the as-prepared DOXY-AuNPs solution was centrifuged at 15.000 rpm for 30 min for three times **to remove the excess of DOXY** and then the supernatant was discarded, and the residue was redispersed in an equivalent amount of water. This was repeated twice.

Doxycycline loading into AuPEG and formation of DOXY IN-AuNPs

Synthesis of DOXY IN-AuNPs colloids included three main steps: (Scheme 1C). 20 mL $HAuCl_4$ solution (8.63×10^{-4} M) was mixed to DOXY (200 µL, 1 mg/mL in water) and aged for 10 min. After 10 min, 1 mL of dicarboxylic PEG was added. Finally, 300 µL of aqueous 0.01 M $NaBH_4$ was added at once. **After 15min of reaction, the as-prepared DOXY-AuNPs solution was centrifuged at 15.000 rpm for 30 min for three times to remove the excess of DOXY and PEG and then the supernatant was discarded, and the residue was redispersed in an equivalent amount of water. This was repeated twice.**

Doxycycline loading onto AuPEG and formation of DOXY ON-AuNPs

Synthesis of pegylated- gold nanoparticles (PEG-AuNPs)

Synthesis of AuPEG Colloids of COOH-terminated PEG-coated AuNPs (PEG-AuNPs) were prepared according to previously described procedure[20] [19] [53] [31]. Briefly, 20 mL of chloroauric acid ($HAuCl_4$) aqueous solution (8.63×10^{-4} M) was added to 0.25 mL of dicarboxylic PEG and mixed by magnetic stirring for 10 minutes at room temperature. To this solution, 6 mL of aqueous 0.01 M $NaBH_4$ was added at once. The color of the dispersion indeed instantly changed from yellow to red when sodium borohydride was added to a solution of gold precursor in the presence of PEG-diacid polymer, confirming the formation of AuPEG in the solution. The as-prepared PEG-Au NP solution was purified by centrifugation to remove excess of non-conjugated dicarboxylic PEG. Centrifugation was carried out at 15,000 rpm for 30 minutes for three times **in order to remove the excess of PEG** and then the supernatant was discarded. The residue was redispersed in an equivalent amount of water. This was repeated twice. Conjugation of DOXY to PEG-AuNPs surface was carried out as from previous published work [19] using a carbodiimide-based conjugation of the

carboxylic-terminated polymer. Briefly, 50 µL of EDC/NHS (40/10 mg ratio) aqueous solution was added to 5 mL of PEG-AuNPs. After 2 hours, DOXY (50 µL, 1mg/mL) was added and aged for 2 hours. The reaction mixture was then centrifuged three times and

redispersed in water to remove any unbound DOXY. The encapsulation efficiency (percentage of DOXY bound to nanoparticles) was calculated as the difference between the initial drug content and the amount of free DOXY in the filtrate after separation of the nanoparticles by ultrafiltration (Ultrafree MC centrifugal filter units, 30,000 NMWL; Merck Millipore, Darmstadt, Germany). The reaction efficiency was equal to 85%.

Physico-chemical characterization

All the measurements were performed in duplicate in order to validate the reproducibility of the synthetic procedure**.**

UV-Vis absorption spectroscopy: All experiments were performed as previously described [19] in water at AuNPs concentration equal to 10^{-4} M.

Transmission Electron microscopy (TEM): All microscopy analysis were realized as previously described[19] [16].

Raman Spectroscopy: The Raman experiments have been performed on an Xplora spectrometer (Horiba Scientifics-France). The Raman spectra have been recorded using an excitation wavelength of 785 nm (diode laser) at room temperature. For measurements in solution, a macro-objective with a focal length of 40 mm (NA = 0.18) was used in backscattering configuration. The achieved spectral resolution is close to 2 cm^{-1}.

Dynamic light scattering (DLS): The size measurements were performed using a Zetasizer Nano ZS (Malvern Instruments, Malvern, UK) equipped with a He-Ne laser (633 nm, fixed scattering angle of 173°) at room temperature.

Zeta potential measurements: All measurements were carried out as previously described [16].

Stability of Doxy gold nanoparticles (DOXY-AuNPs, DOXY IN-AuNPs, DOXY ON-AuNPs) as a function of pH.

For stability studies, all nanoparticles were dispersed in bacterial culture media (0.1 M; pH 8), and absorption spectra collected over 3 months (**Figure S1 Supporting Informations**).

DOXY loading efficiency: The amount of the antibiotic incorporated into PEG-AuNPs was measured by UV-Vis absorption spectroscopy. Absorption at 350-275 nm was used to extrapolate DOXY concentrations based on a calibration curve (**Figure S2 in the Supporting Information**). Because the AuNPs spectrum could interfere with DOXY detection, the DOXY loading efficiency was calculated as follows (**Equation 1**):

$$DOXY\ loading\ efficiency\ (\%) = \frac{C_1 - C_2}{C_1} \times 100 \quad \textbf{Equation 1}$$

Where C_1 is the initial drug content and C_2 is the amount of free doxorubicin in the filtrate[16].

Antimicrobial Assay

Bacterial strains

Enterococcus faecalis UCN41, *Enterococcus faecium* BM4147 and ATCC®19434T™, *Klebsiella pneumoniae* ATCC®700603™, *Escherichia coli* ATCC®25922™, *Acinetobacter baumannii* CIP7010, and *Pseudomonas aeuginosa* PAO1 strains were used as reference strains [46, 54]. *P. aeruginosa* clinical isolates were isolated from blood culture and tracheal aspirates at the teaching hospital of Besançon, France (CHRU Jean Minjoz). Well-characterized *P. aeruginosa* strains from the collection of the French National Reference Centre (NRC) for Antibiotic Resistance were also included in the study to evaluate the activity of the synthetized compounds derivative

from **DOXY**. The collection included 15 well-characterized resistant *P. aeruginosa* strains, of which 6 were carbapenems producers including 3 VIM-2, one IMP-13, one IMP-15, and one NDM-1, 4 Extended-Spectrum ß-Lactamases (ESBL) producers including (GES-1, PER-1, SHV-2a, and VEB-1a), and 5 AmpC overproducers.

Susceptibility testing

The minimum inhibitory concentrations (MICs) of the selected strains were determined by microdilution method in Mueller Hinton Broth (MHB, Becton Dickinson, Le Pont de Claix, France) containing adjusted concentrations of Ca^{2+} (from 20 to 25 mg/L) and Mg^{2+} (from 10 to 12.5 mg/L) according to Clinical and Laboratories Standards Institute recommendations [55]. Briefly, from fresh bacterial cultures, microplates were inoculated with 10^5 CFU/mL in MHB containing serial dilutions of molecules and incubated at 35°C for 18h. MICs of the molecules tested were compared to antibiotics usually used as reference according to the species. MICs were defined as the lowest concentration of antibiotic that completely inhibits visible growth after 24 h of incubation at 35°C. MICs of indicated antibiotics and molecules were determined in triplicate.

3. CONCLUSION

In this study, we described a new approach to synthetize new antibacterial nanotherapeutics based on stable DOXY–gold nanoparticles. Chemical physics characterizations were extensively achieved and fully elucidated the formation mechanism of the nanostructure and the DOXY conformational changes associated with such processes. Infact, the amine group of DOXY acts as both a reducing and stabilizing agent and therefore the antibacterial activity of DOXY is preserved due to the presence of the free β lactam ring being available on the surface of the nanoparticles. The capping agents aren't needed on the surface of nanoparticles due to block potential adsorption surface sites. However, we have shown that PEG played a key role in the loading of DOXY around the particle, which culminated in an increased bactericidal activity towards major human pathogens (*Staphylococcus aureus*, *Escherichia coli*, *Klebsiella pneumoniae*, *Pseudomonas aeruginosa*, and *Acinetobacter baumannii*). Thus, **DOXY** -loaded nanoparticles could be used efficiently for antibacterial therapy, against a variety number of bacterial species. Given these best-quality results, this antibiotic system based on doxycicline constitutes a real promise as a therapeutic entity in disease treatment. Further studies are still envisaged, focused on *no-cycline-cycline hybrid antibiotic nanoparticles* in order to improve the selectivity and efficacy of the antibacterial system.

ASSOCIATED CONTENT

Supporting Information. Supplementary figures, schemes and tables are provided. This material is available free of charge *via* the Internet at http://.....

Corresponding Author

*jolanda.spadavecchia@univ-paris13.fr

ACKNOWLEDGMENT

This work was supported by project from the Centre National of Recherche (CNRS) and Univ-Paris13

Reference :

[1] M. Exner, S. Bhattacharya, B. Christiansen, J. Gebel, P. Goroncy-Bermes, P. Hartemann, P. Heeg, C. Ilschner, A. Kramer, E. Larson, W. Merkens, M. Mielke, P. Oltmanns, B. Ross, M. Rotter, R. M. Schmithausen, H.-G. Sonntag, M. Trautmann, *GMS Hygiene and Infection Control* **2017**, *12*, Doc05.
[2] M. J. Silvero C, D. M. Rocca, E. A. de la Villarmois, K. Fournier, A. E. Lanterna, M. F. Pérez, M. C. Becerra, J. C. Scaiano, *ACS Omega* **2018**, *3*, 1220-1230.
[3] A. Rai, A. Prabhune, C. C. Perry, *Journal of Materials Chemistry* **2010**, *20*, 6789-6798.
[4] R. Misra, S. K. Sahoo, *Methods Enzymol* **2012**, *509*, 61-85.
[5] H. F. O. Silva, K. M. G. Lima, M. B. Cardoso, J. F. A. Oliveira, M. C. N. Melo, C. Sant'Anna, M. Eugênio, L. H. S. Gasparotto, *RSC Advances* **2015**, *5*, 66886-66893.
[6] N. F. Cover, S. Lai-Yuen, A. K. Parsons, A. Kumar, *Int J Nanomedicine* **2012**, *7*, 2411-2419.
[7] P. Liu, H. Wang, J. K. Hiltunen, Z. Chen, J. Shen, *Particle & Particle Systems Characterization* **2015**, *32*, 749-755.
[8] D. Cheng, M. Yu, F. Fu, W. Han, G. Li, J. Xie, Y. Song, M. T. Swihart, E. Song, *Analytical Chemistry* **2016**, *88*, 820-825.
[9] J. Kreuter, *Infection* **1991**, *19*, S224-S228.
[10] H. Pinto-Alphandary, A. Andremont, P. Couvreur, *International journal of antimicrobial agents* **2000**, *13*, 155-168.
[11] H. Gu, P. L. Ho, E. Tong, L. Wang, B. Xu, *Nano Letters* **2003**, *3*, 1261-1263.
[12] B. Saha, J. Bhattacharya, A. Mukherjee, A. Ghosh, C. Santra, A. K. Dasgupta, P. Karmakar, *Nanoscale Research Letters* **2007**, *2*, 614.
[13] H. Deng, D. McShan, Y. Zhang, S. S. Sinha, Z. Arslan, P. C. Ray, H. Yu, *Environmental science & technology* **2016**, *50*, 8840-8848.
[14] N. Joshi, D. Q. Miller, *Arch Intern Med* **1997**, *157*, 1421-1428.
[15] B. A. Cunha, P. Domenico, C. B. Cunha, *Clin Microbiol Infect* **2000**, *6*, 270-273.

[16] H. Moustaoui, D. Movia, N. Dupont, N. Bouchemal, S. Casale, N. Djaker, P. Savarin, A. Prina-Mello, M. L. de la Chapelle, J. Spadavecchia, *ACS Applied Materials & Interfaces* **2016**, *8*, 19946-19957.

[17] A. O. Legendre, L. R. R. Silva, D. M. Silva, I. M. L. Rosa, L. C. Azarias, P. J. de Abreu, M. B. de Araújo, P. P. Neves, C. Torres, F. T. Martins, A. C. Doriguetto, *CrystEngComm* **2012**, *14*, 2532-2540.

[18] M. Zilberman, J. J. Elsner, *Journal of Controlled Release* **2008**, *130*, 202-215.

[19] J. Spadavecchia, D. Movia, C. Moore, C. M. Maguire, H. Moustaoui, S. Casale, Y. Volkov, A. Prina-Mello, in *Int J Nanomedicine, Vol. 11*, **2016**, pp. 791-822.

[20] J. Spadavecchia, R. Perumal, A. Barras, J. Lyskawa, P. Woisel, W. Laure, C. M. Pradier, R. Boukherroub, S. Szunerits, *The Analyst* **2014**, *139*, 157-164.

[21] A. Fakhri, S. Tahami, M. Naji, *Journal of Photochemistry and Photobiology B: Biology* **2017**, *169*, 21-26.

[22] R. Jagannathan, P. Poddar, A. Prabhune, *The Journal of Physical Chemistry C* **2007**, *111*, 6933-6938.

[23] X. Peng, J. Wickham, A. P. Alivisatos, *Journal of the American Chemical Society* **1998**, *120*, 5343-5344.

[24] S. S. Shankar, S. Bhargava, M. Sastry, *Journal of nanoscience and nanotechnology* **2005**, *5*, 1721-1727.

[25] S. K. Nune, N. Chanda, R. Shukla, K. Katti, R. R. Kulkarni, S. Thilakavathi, S. Mekapothula, R. Kannan, K. V. Katti, *Journal of materials chemistry* **2009**, *19*, 2912-2920.

[26] M. Gwendolyn, M. Hanane, H. M. Ben, D. Nadia, C. M. Lamy, S. Jolanda, *Particle & Particle Systems Characterization* **2018**, *35*, 1700299.

[27] L. Hui, J. Peng, L. Zhonghu, L. Xiaowu, D. Nadia, S. Jolanda, *Particle & Particle Systems Characterization*, *0*, 1800082.

[28] B. A. Cunha, C. M. Sibley, A. M. Ristuccia, *Ther Drug Monit* **1982**, *4*, 115-135.

[29] I. Chopra, M. Roberts, *Microbiol Mol Biol Rev* **2001**, *65*, 232-260.

[30] S. Link, M. A. El-Sayed, *The Journal of Physical Chemistry B* **1999**, *103*, 8410-8426.

[31] J. Spadavecchia, E. Apchain, M. Alberic, E. Fontan, I. Reiche, *Angewandte Chemie (International ed. in English)* **2014**, *53*, 8363-8366.

[32] P. K. Jain, K. S. Lee, I. H. El-Sayed, M. A. El-Sayed, *The Journal of Physical Chemistry B* **2006**, *110*, 7238-7248.

[33] aH. Moustaoui, D. Movia, N. Dupont, N. Bouchemal, S. Casale, N. Djaker, P. Savarin, A. Prina-Mello, M. L. de la Chapelle, J. Spadavecchia, *ACS applied materials & interfaces* **2016**, *8*, 19946-19957; bJ. Politi, L. De Stefano, S. Longobardi, P. Giardina, I. Rea, C. Methivier, C. M. Pradier, S. Casale, J. Spadavecchia, *Colloids and surfaces. B, Biointerfaces* **2015**, *136*, 214-221; cJ. Spadavecchia, D. Movia, C. Moore, C. M. Maguire, H. Moustaoui, S. Casale, Y. Volkov, A. Prina-Mello, *International journal of nanomedicine* **2016**, *11*, 791-822.

[34] G. Marguerit, H. Moustaoui, M. B. Haddada, N. Djaker, M. L. Chapelle, J. Spadavecchia, *Particle & Particle Systems Characterization* **2018**, *35*, 1700299.

[35] I. M. Redelsperger, T. Taldone, E. R. Riedel, M. L. Lepherd, N. S. Lipman, F. R. Wolf, *Journal of the American Association for Laboratory Animal Science : JAALAS* **2016**, *55*, 467-474.

[36] R. K. Franklin, S. A. Marcus, A. M. Talaat, B. K. KuKanich, R. Sullivan, L. A. Krugner-Higby, T. D. Heath, *Drug Metabolism and Disposition* **2015**, *43*, 1236-1245.

[37] A. Omri, M. Ravaoarinoro, *International journal of antimicrobial agents* **1996**, *7*, 9-14.

[38] G. Budai, G. Maróti, R. Dekker, D. Huisman, L. Kroon, *Journal of Scheduling* **2010**, *13*, 281-297.

[39] I. V. Zhigaltsev, N. Maurer, K. Edwards, G. Karlsson, P. R. Cullis, *Journal of Controlled Release* **2006**, *110*, 378-386.

[40] W. Tu, X. Xu, L. Peng, X. Zhong, W. Zhang, M. M. Soundarapandian, C. Balel, M. Wang, N. Jia, W. Zhang, F. Lew, S. L. Chan, Y. Chen, Y. Lu, *Cell* **2010**, *140*, 222-234.

[41] I. Capek, *Advances in colloid and interface science* **2017**.

[42] I. Chopra, M. Roberts, *Microbiology and Molecular Biology Reviews* **2001**, *65*, 232-260.

[43] D. E. Brodersen, W. M. Clemons, A. P. Carter, R. J. Morgan-Warren, B. T. Wimberly, V. Ramakrishnan, *Cell* **2000**, *103*, 1143-1154.

[44] C. Marambio-Jones, E. M. V. Hoek, *Journal of Nanoparticle Research* **2010**, *12*, 1531-1551.

[45] aH. W. Boucher, G. H. Talbot, D. K. Benjamin, Jr., J. Bradley, R. J. Guidos, R. N. Jones, B. E. Murray, R. A. Bonomo, D. Gilbert, A. Infectious Diseases Society of, *Clin Infect Dis* **2013**, *56*, 1685-1694; bD. M. Shlaes, D. Sahm, C. Opiela, B. Spellberg, *Antimicrobial Agents and Chemotherapy* **2013**, *57*, 4605-4607.
[46] T. D. Bugg, G. D. Wright, S. Dutka-Malen, M. Arthur, P. Courvalin, C. T. Walsh, *Biochemistry* **1991**, *30*, 10408-10415.
[47] H. S. Sader, D. J. Farrell, R. K. Flamm, R. N. Jones, *Int J Antimicrob Agents* **2014**, *43*, 328-334.
[48] P. D. Lister, D. J. Wolter, N. D. Hanson, *Clin Microbiol Rev* **2009**, *22*, 582-610.
[49] C. Juan, G. Torrens, M. Gonzalez-Nicolau, A. Oliver, *FEMS Microbiol Rev* **2017**, *41*, 781-815.
[50] A. Potron, L. Poirel, P. Nordmann, *Int J Antimicrob Agents* **2015**, *45*, 568-585.
[51] A. P. Magiorakos, A. Srinivasan, R. B. Carey, Y. Carmeli, M. E. Falagas, C. G. Giske, S. Harbarth, J. F. Hindler, G. Kahlmeter, B. Olsson-Liljequist, D. L. Paterson, L. B. Rice, J. Stelling, M. J. Struelens, A. Vatopoulos, J. T. Weber, D. L. Monnet, *Clin Microbiol Infect* **2012**, *18*, 268-281.
[52] H. Bajaj, S. Acosta Gutierrez, I. Bodrenko, G. Malloci, M. A. Scorciapino, M. Winterhalter, M. Ceccarelli, *ACS Nano* **2017**, *11*, 5465-5473.
[53] V. Melani, M. B. Haddada, H. Moustaoui, J. Landoulsi, N. Djaker, M. L. de la Chapelle, J. Spadavecchia, *Frontiers in Laboratory Medicine* **2017**, *1*, 114-121.
[54] aP. G. P. Bouvet, *Int. J. Syst. Bacteriol.* **1986**, 228-240; bC. K. Stover, X. Q. Pham, A. L. Erwin, S. D. Mizoguchi, P. Warrener, M. J. Hickey, F. S. L. Brinkman, W. O. Hufnagle, D. J. Kowalik, M. Lagrou, R. L. Garber, L. Goltry, E. Tolentino, S. Westbrock-Wadman, Y. Yuan, L. L. Brody, S. N. Coulter, K. R. Folger, A. Kas, K. Larbig, R. Lim, K. Smith, D. Spencer, G. K.-S. Wong, Z. Wu, I. T. Paulsen, J. Reizer, M. H. Saier, R. E. W. Hancock, S. Lory, M. V. Olson, *Nature (London)* **2000**, *406*, 959-964.
[55] CLSI, Clinical and Laboratory Standards Institute, Wayne, PA, **2017**.

Figures and scheme

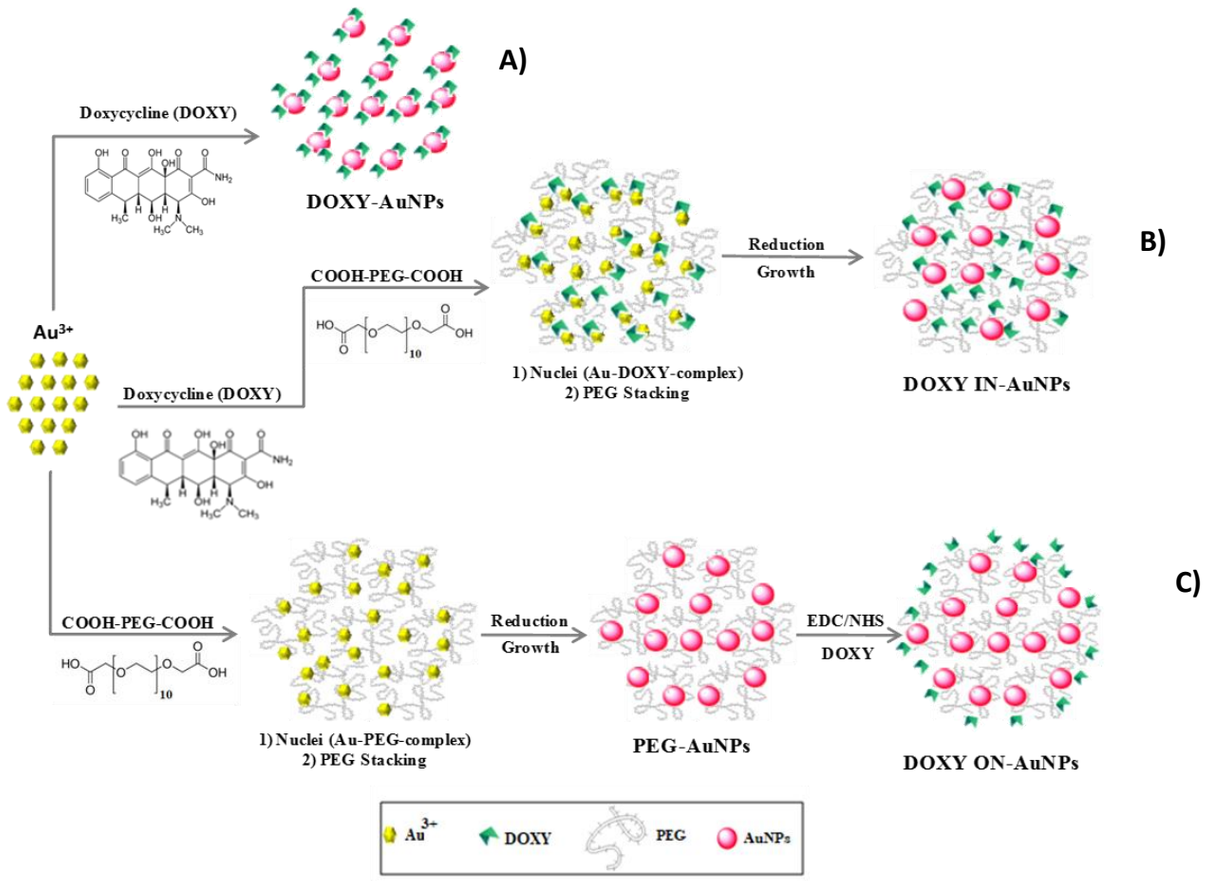

Scheme 1. Schematic representation of two possible mechanisms for the synthesis of DOXY-AuNPs, DOXY IN-AuNPs and DOXY ON-AuNPs. It should be noted that the scheme is not to scale.

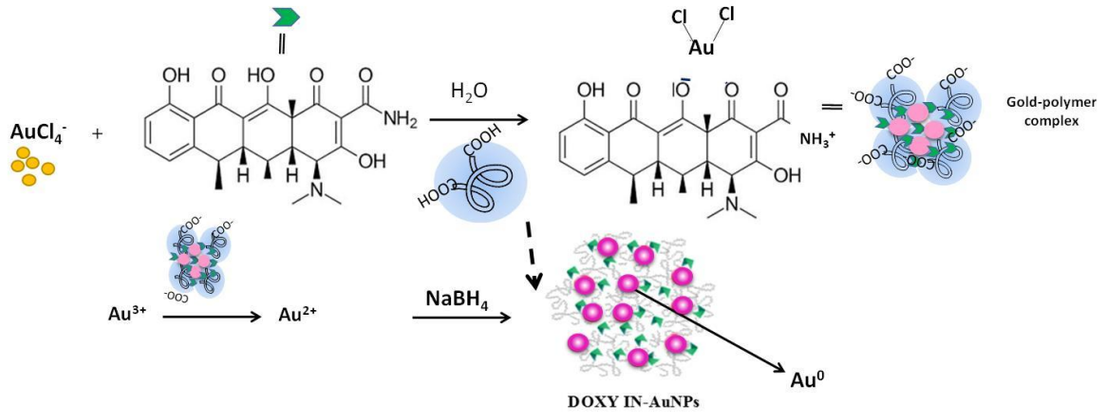

Scheme 2: Schematic of proposed mechanism of $AuCl_4^-$ reduction and particle formation in the presence of DOXY as surfactant (Please note that drawings are not in scale and are not intended to be representative of the full samples composition).

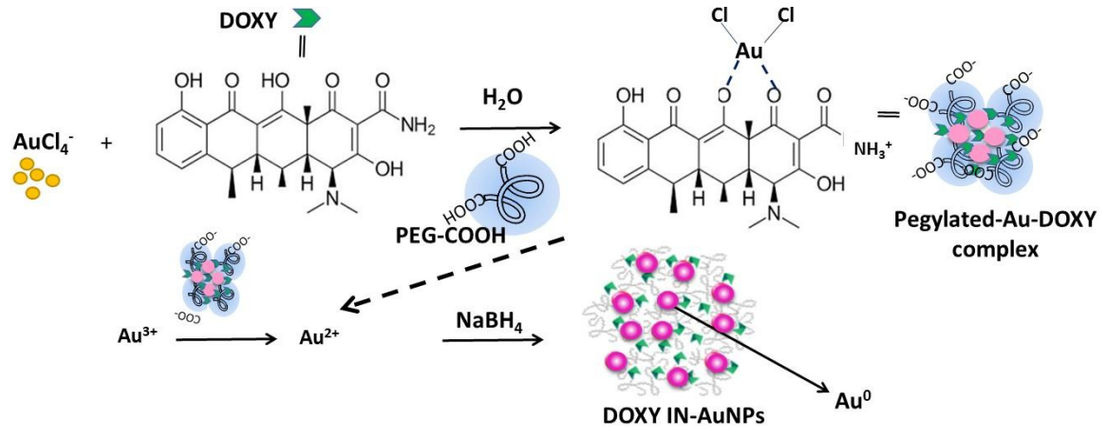

Scheme 3: Schematic of proposed mechanism of $AuCl_4^-$ reduction and particle formation in the presence of DOXY and PEG-diacid as surfactants (Please note that drawings are not in scale and are not intended to be representative of the full samples composition).

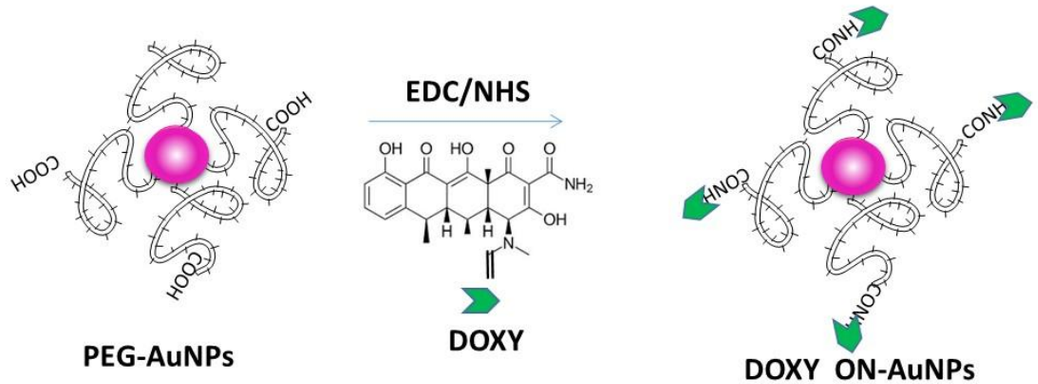

Scheme 4: Representation of Doxycicline conjugation onto PEG-AuNPs by carbodiimide chemistry (Please note that drawings are not in scale and are not intended to be representative of the full samples composition).

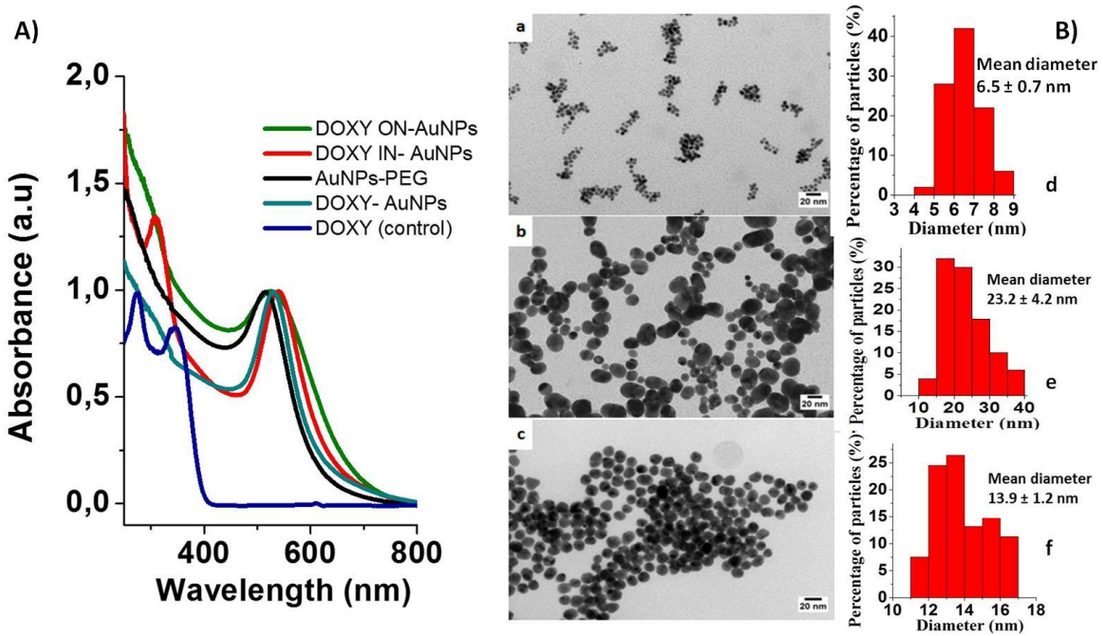

Figure 1. A) UV-Vis spectra of the prepared AuNPs. B) TEM images and size distribution of the prepared DOXY-AuNPs (a,d), DOXY IN-AuNPs (b,e) and DOXY ON-AuNPs (c,f).

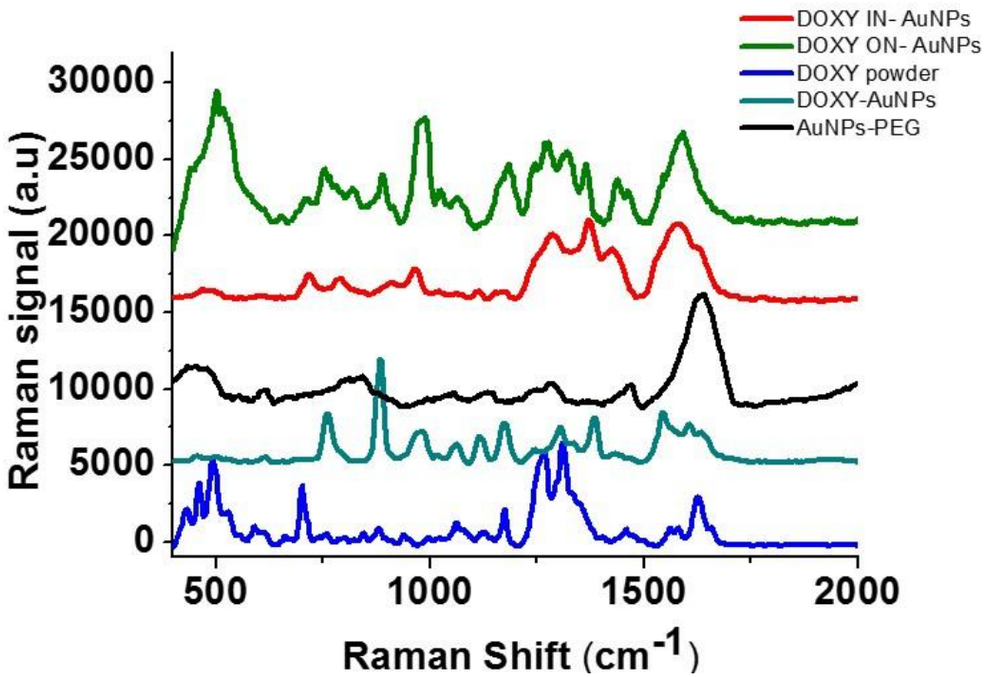

Figure 2. .Raman spectra of DOXY-AuNPs, DOXY IN-AuNPs and DOXY ON-AuNPs, DOXY powder and COOH-terminated PEG (PEG-COOH) are also reported for comparison. Experimental conditions: λexc = 785 nm; laser power 20 mW; 600 T of 120 s.

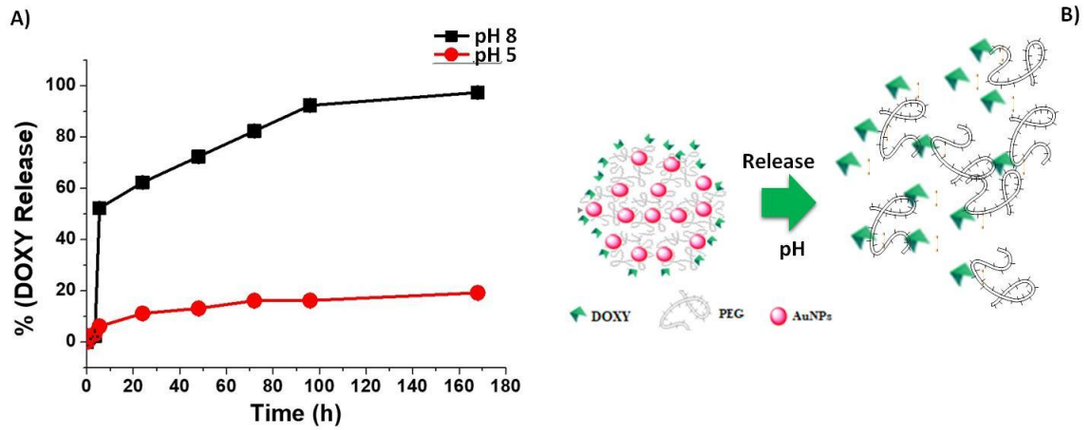

Figure 3: A) Drug release percentage (%) of DOXY ON AuNPs time in PBS (37 °C) at pH = 5.0 or at pH = 8.0. **B)** Schematic diagram of DOXY release under pH conditions.

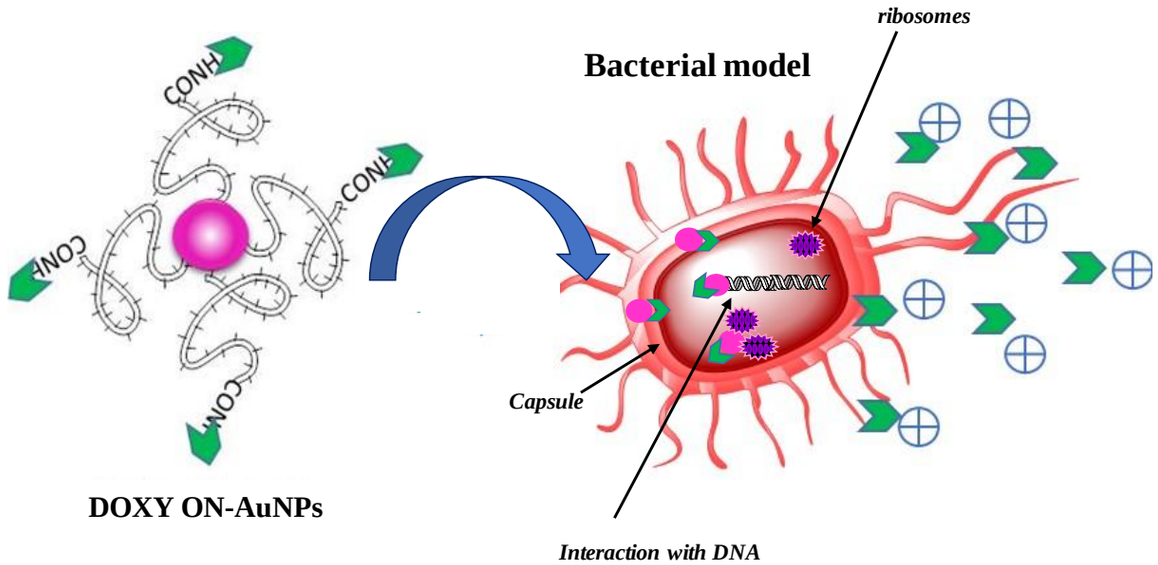

Scheme 4: Scheme summarizing DOXY ON-AuNPs interaction with bacterial cells. (Please note that drawings are not in scale and are not intended to be representative of the full samples composition).

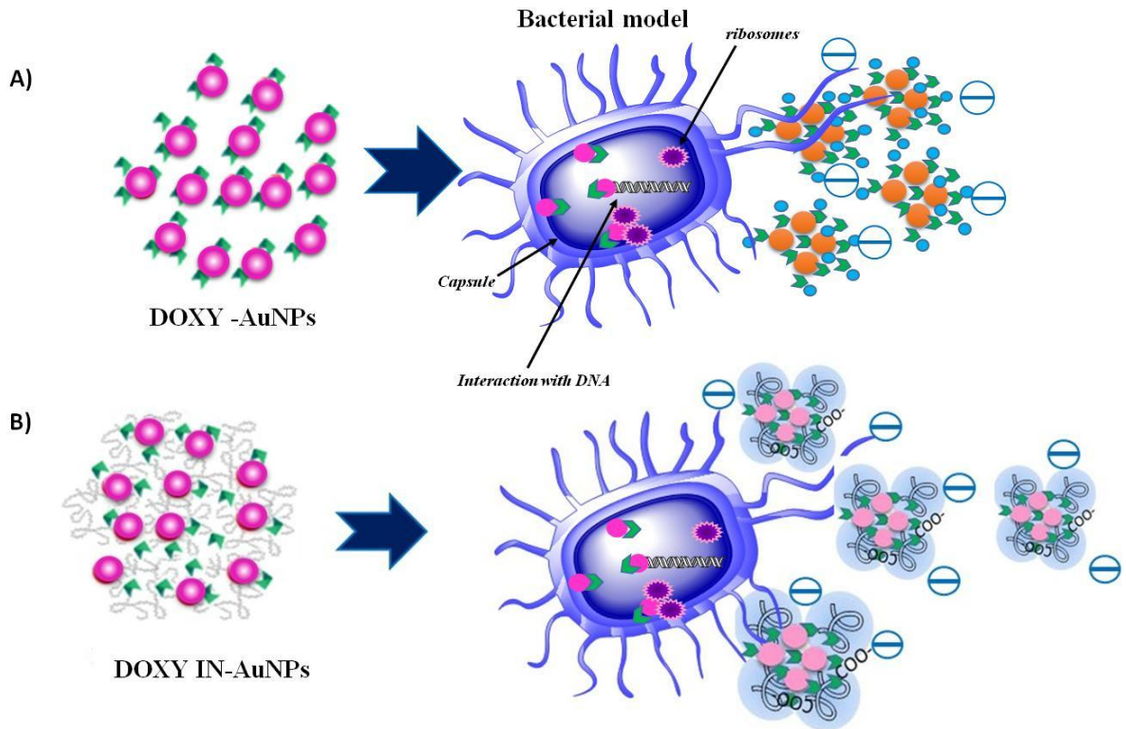

Scheme 5: Scheme summarizing **DOXY IN-AuNPs** (panel A) and **DOXY IN-AuNPs** (panel B) interaction with bacterial cells. (Please note that drawings are not in scale and are not intended to be representative of the full samples composition).

Supporting Information

Novel synthesis and characterization of doxycycline-loaded gold nanoparticles. The golden doxycycline for antibacterial applications.

Maroua Ben Haddada[1], Katy Jeannot[2], Jolanda Spadavecchia[1]*

[1] *CNRS, UMR 7244, CSPBAT, Laboratoire de Chimie, Structures et Propriétés de Biomateriaux et d'Agents Therapeutiques Université Paris 13, Sorbonne Paris Cité, Bobigny, France*

[2] *Laboratoire de Bactériologie, Centre National de Référence (CNR) de la Résistance aux Antibiotiques, Centre Hospitalier Régional Universitaire (CHRU) de Besançon, UMR4269 "Chrono-Environnement", Boulevard Fleming, 25030 Besançon, France.*

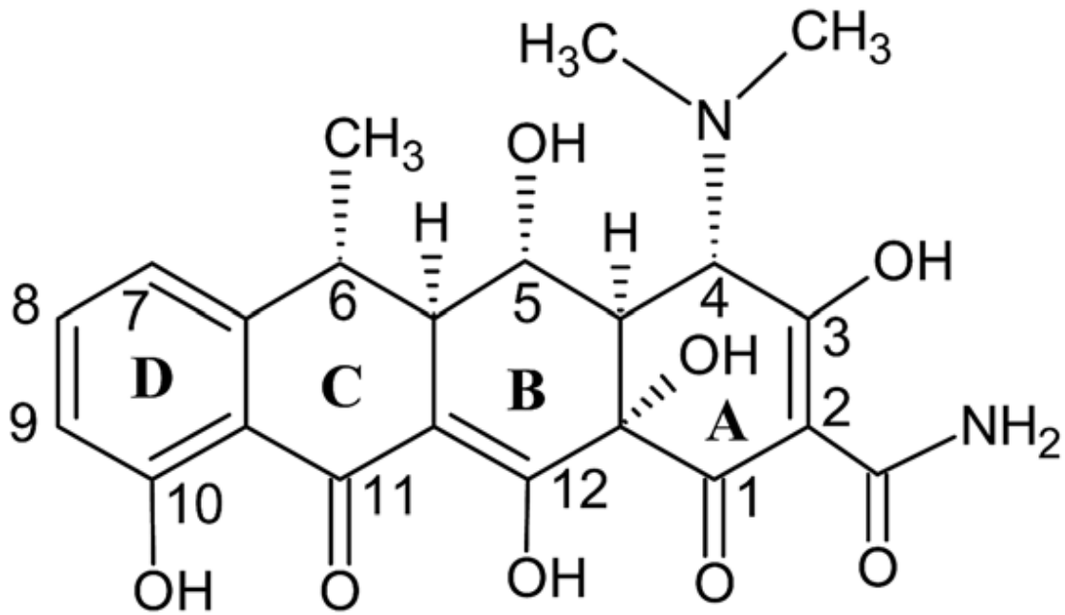

Scheme S1: Chemical structure of doxycicline (DOXY).Rings are identified with letters from A to D; this nomenclature is used for Raman band assignments.

Table 1. Average hydrodynamic diameter and zeta potential of the prepared nanoparticles.
Note: Data are reported as mode ± standard deviation.

Particles	Particle size (nm)	PDI	Zeta potential (mV)
DOXY-AuNPs	11.59 ± 0.3	0.266	-34.70 ± 0.8
DOXY IN-AuNPs	70.29 ±0.5	0.330	-17.93 ± 0.7
DOXY ON-AuNPs	19.94 ± 0.6	0.238	-25.60 ± 0.5

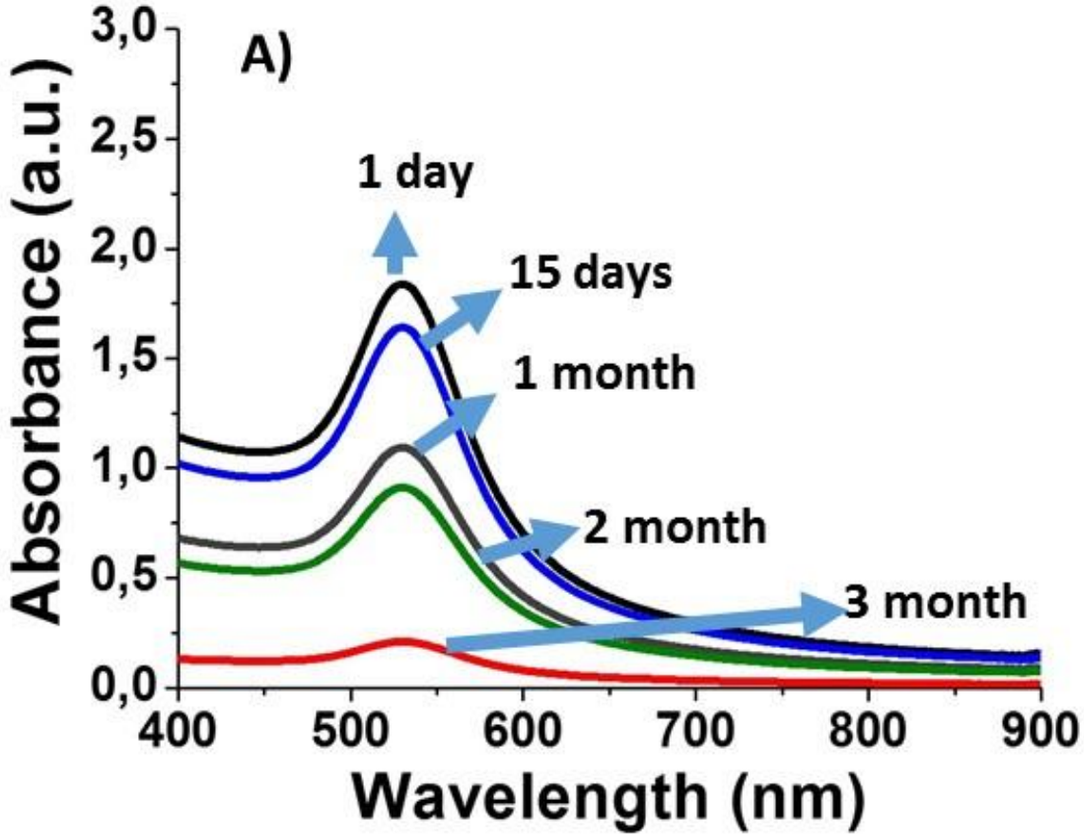
A)
1 day
15 days
1 month
2 month
3 month
Absorbance (a.u.)
Wavelength (nm)
3,0
2,5
2,0
1,5
1,0
0,5
0,0
400
500
600
700
800
900

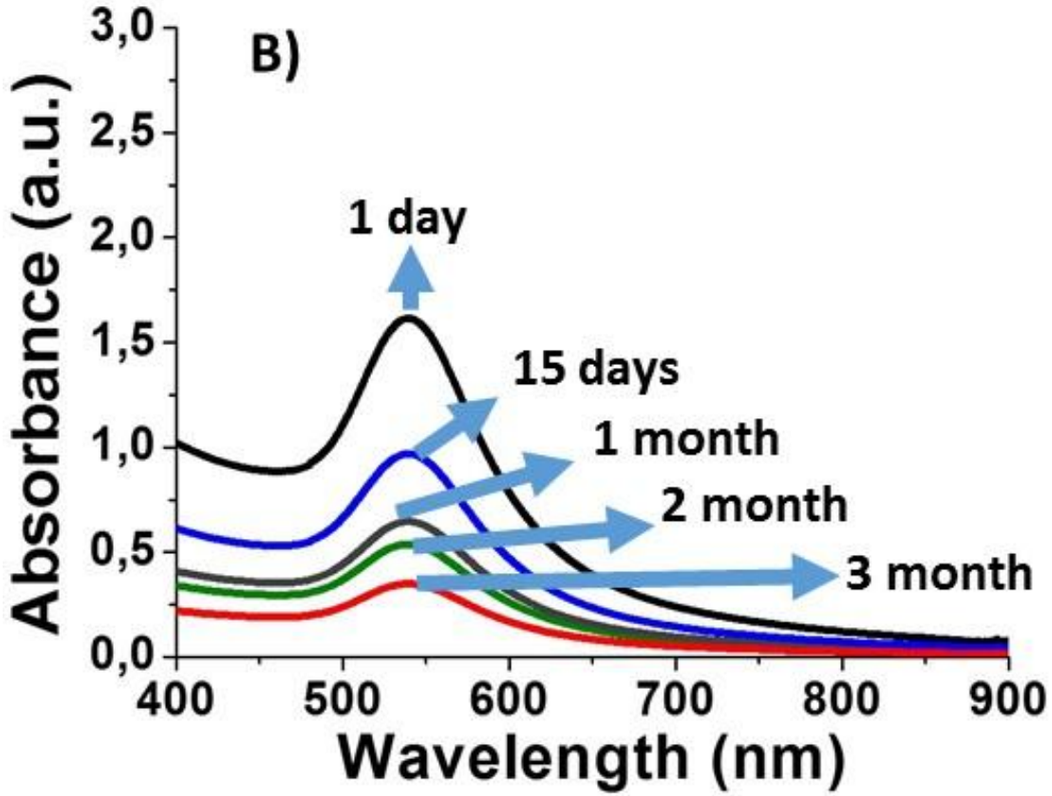
B)
Absorbance (a.u.)
3,0
2,5
2,0
1,5
1,0
0,5
0,0
400
500
600
700
800
900
Wavelength (nm)
1 day
15 days
1 month
2 month
3 month

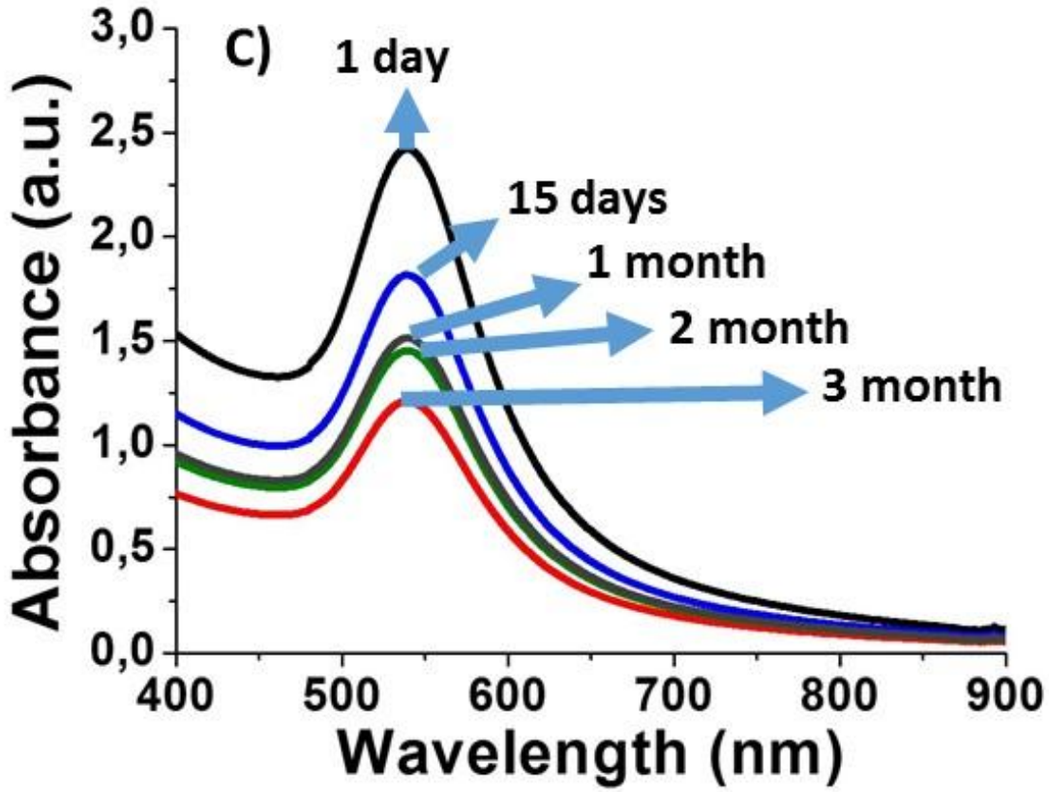

Figure S1: Changes in the UV-Vis absorption spectra of DOXY gold nanoparticles when incubated in bacterial culture media solution at pH 8, up to three months (A: DOXY AuNPs; B: DOXY IN AuNPs; C: DOXY ON AuNPs) .

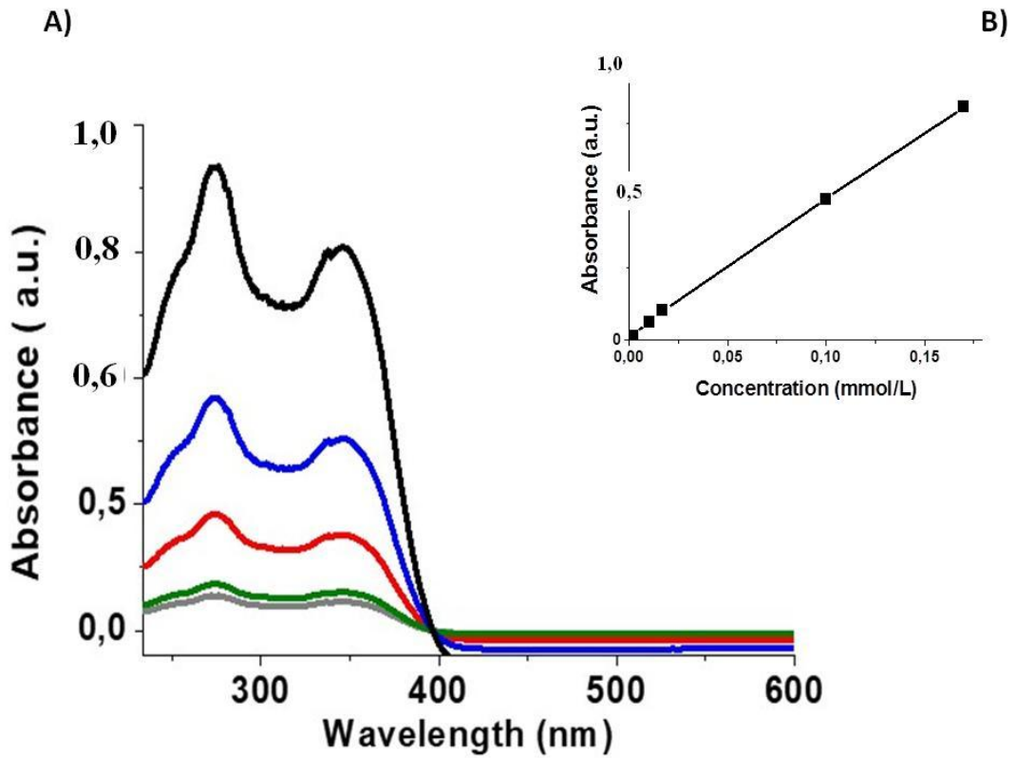

Figure S2: (**a**) UV-Vis absorption spectra of DOXY at increasing known concentrations. (**b**) A calibration curve (R^2 = 0.9997) was extrapolated from such measurements. The amount of DOXY molecules contained into DOXY ON AuNPs, DOXY IN AuNPS and DOXY AuNPs were estimated based on this curve.